

The Outer Limits of Galaxy Clusters: Observations to the Virial Radius with Suzaku, XMM, and Chandra

Eric D. Miller^{*}, Marshall Bautz^{*}, Jithin George[†], Richard Mushotzky[†],
David Davis^{**},[‡] and J. Patrick Henry[§]

^{*}MIT Kavli Institute for Astrophysics and Space Research, Cambridge, MA, USA;
milleric@mit.edu

[†]Astronomy Department, University of Maryland, College Park, MD, USA

^{**}CRESSST and X-ray Astrophysics Laboratory, NASA/GSFC, Greenbelt, MD, USA

[‡]Department of Physics, University of Maryland Baltimore County, Baltimore, MD, USA

[§]Institute for Astronomy, University of Hawaii, Honolulu, HI, USA

Abstract. The outskirts of galaxy clusters, near the virial radius, remain relatively unexplored territory and yet are vital to our understanding of cluster growth, structure, and mass. In this presentation, we show the first results from a program to constrain the state of the outer intra-cluster medium (ICM) in a large sample of galaxy clusters, exploiting the strengths of three complementary X-ray observatories: *Suzaku* (low, stable background), *XMM-Newton* (high sensitivity), and *Chandra* (good spatial resolution). By carefully combining observations from the cluster core to beyond r_{200} , we are able to identify and reduce systematic uncertainties that would impede our spatial and spectral analysis using a single telescope. Our sample comprises nine clusters at $z \sim 0.1$ – 0.2 fully covered in azimuth to beyond r_{200} , and our analysis indicates that the ICM is not in hydrostatic equilibrium in the cluster outskirts, where we see clear azimuthal variations in temperature and surface brightness. In one of the clusters, we are able to measure the diffuse X-ray emission well beyond r_{200} , and we find that the entropy profile and the gas fraction are consistent with expectations from theory and numerical simulations. These results stand in contrast to recent studies which point to gas clumping in the outskirts; the extent to which differences of cluster environment or instrumental effects factor in this difference remains unclear. From a broader perspective, this project will produce a sizeable fiducial data set for detailed comparison with high-resolution numerical simulations.

Keywords: Galaxy Clusters, ICM, Suzaku, X-ray

PACS: 95.85.Nv 98.65.Cw 98.65.Hb

CLUSTER OUTSKIRTS: THE FINAL FRONTIER

Exploring the outskirts of galaxy clusters is vital to our understanding of cluster growth, structure, and mass. The region near the boundary of the dynamically relaxed cluster volume ($\sim r_{200}$ [1]), offers a direct view of cluster growth and ICM accretion [2]. Simulations predict deviations from hydrostatic equilibrium in the outskirts of clusters at scales on the order of $r_{2500} < r < r_{200}$, well beyond the influence of cooling and AGN feedback processes in the cluster core [3, 4]. Moreover, it may be that signatures of spatially inhomogeneous accretion from cosmic filaments are observable at these radii. X-ray observations of clusters at $r > r_{500}$ also probe the distribution of mass to large radii, and in so doing provide new constraints on structure formation models [5, 6, 3]. Finally, accurate knowledge of the mass and baryonic fraction of clusters is essential for

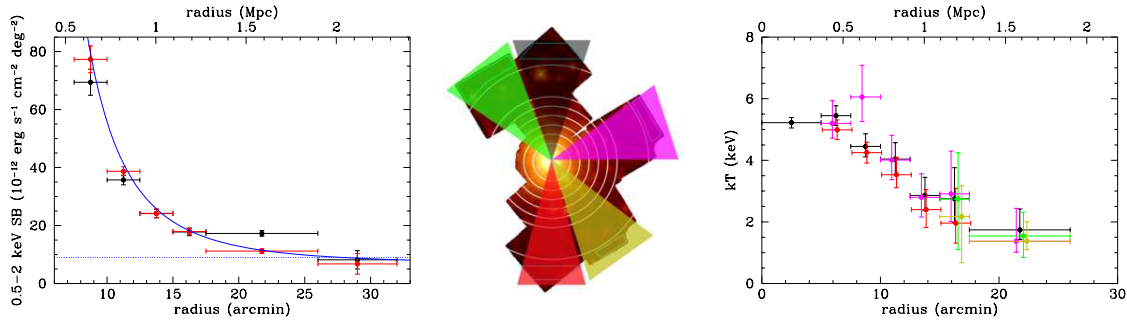


FIGURE 1. Abell 1795 surface brightness (left) and temperature profiles (right). The image (center) shows color-coding for the radial directions probed; for clarity, only the North and South directions are shown in the surface brightness profile. A $4\text{-}\sigma$ difference is seen in the surface brightness between the North and South [9], and a rapid decline in temperature is seen toward all directions.

cluster-based cosmological tests [7, 8]. Accurate cluster masses within r_{500} , for example, required for many cosmological tests, rely on knowledge of both the temperature and its radial gradient at r_{500} , and observations to larger radius are essential to determine these quantities reliably.

Spatially resolved X-ray spectroscopy is one of the prime methods for mapping the distribution of mass and intracluster plasma, and it is the only way to measure heavy elements in the gas in galaxy clusters. Although *Chandra* and *XMM* have successfully probed the central regions of clusters [10, 11, 12], these instruments have difficulty observing the faint emission near r_{200} due to their relatively high and time-variable background, and in fact conditions in the ICM beyond $\sim 0.5r_{200}$ have not been well studied by these observatories. *Suzaku*'s low and stable background and substantial effective area, however, have already enabled observations of a handful of clusters that have successfully detected ICM emission out to and even beyond r_{200} [13, 14, 9, 15, 16, 17, 18]. Our own *Suzaku* observations of Abell 1795 [9] find significant deviations from hydrostatic equilibrium within $r_{2500}\text{--}r_{200}$, in a cluster which appears to be relaxed at smaller radii. These results point to a rapidly declining temperature profile (see Figure 1), an entropy profile that is flatter than predicted for simple hierarchical structure formation [2], and clearly asymmetric temperature and density profiles at large radius. The steep profile may in turn result from cool, low-entropy infalling substructure, as suggested by the simulations of Roncarelli et al. [3]. Indeed, Burns et al. [4] successfully reproduce with hydrodynamic simulations the temperature and entropy profiles seen in Abell 1795, suggesting that bulk flows and turbulence from accretion greatly affect the energetics of the outer ICM.

TOWARD A LARGE SAMPLE OF CLUSTERS WITH *SUZAKU*

While the previous results are intriguing, the *Suzaku* sample has been small and it is unclear whether it represents clusters generally. Starting in 2010, we have embarked on a comprehensive program of observations of a large sample of clusters with *Suzaku*, utilizing a recent *XMM* cluster survey [12]. This survey is the largest sample of galaxy

TABLE 1. Cluster sample

Cluster	z	kT^* (keV)	r_{200} (arcmin)	t_{exp}^\dagger (ksec)	date obs.
A 383	0.187	5.3	9.3	110	July 2010
A 773	0.216	7.2	9.5	200	May 2011
A 1068	0.147	4.7	10.8	200	Oct 2011
A 1413	0.135	7.6	14.8	170	May 2010 + archive
A 1795	0.063	5.3	26.0	260	June 2009 + archive
A 1914	0.174	11.5	14.5	160	June 2010
A 2204	0.151	8.6	11.8	140	Sept 2010 + archive
A 2667	0.221	8.3	10.0	200	July 2011
RXCJ 0605	0.137	5.2	12.2	150	May 2010

* Average kT from [12]

† Total *Suzaku* exposure time from all pointings.

clusters that have been probed to $\sim r_{500}$, and it is the first sample large enough to find temperature profiles that seem to differ significantly from theoretical predictions [19]. With *Suzaku*, we are able to capitalize on this work by extending the radial coverage beyond that provided by *XMM* to r_{200} , and provide robust, independent checks of the *XMM* results at smaller radii. The goals of this *Suzaku* project are to (1) determine the temperature and density profiles to large radius for a representative sample of apparently relaxed clusters, including those discrepant with numerical simulations; (2) search for azimuthal variations at large radius which may be indicative of the ongoing cluster accretion process; and (3) provide a fiducial data set for detailed comparison with high resolution numerical simulations.

To define our sample we first selected objects with high-quality *XMM* data to approximately r_{500} . This resulted in a sample with a variety of temperature profiles that were falling, flat, or rising in the outer regions. The sample was further restricted using a numerical asymmetry parameter to select clusters that appear relaxed in the *XMM* images. To maximize *Suzaku* observing efficiency, we further selected clusters with $r_{200} \lesssim 17$ arcmin, so that the entire cluster volume within r_{200} could be observed in no more than four overlapping XIS pointings, while allowing sufficient area beyond r_{200} for background estimation. Clusters were eliminated if they were too compact for the ~ 2 arcmin *Suzaku* PSF ($r_{200} \lesssim 9$ arcmin), or if they were so centrally bright so that the scattered light from the core would dominate cluster emission in the r_{500} – r_{200} region. The current sample of 9 clusters is shown in Table 1; it includes Abell 1795, which does not fully meet the criteria outlined above, but has extensive *Suzaku* data from our previous work. We also include two clusters (Abell 1413 and Abell 2204) which have single pointings from the archive; these data have been published [14, 15].

An example cluster is shown in Figure 2, with the projected temperature and surface brightness profiles for Abell 2204 plotted along four radial directions. The temperature drops off rapidly in each direction, although there are differences from pointing to pointing. Both the temperature and surface brightness are well-matched in the overlap region to the *XMM* results, which are azimuthally averaged.

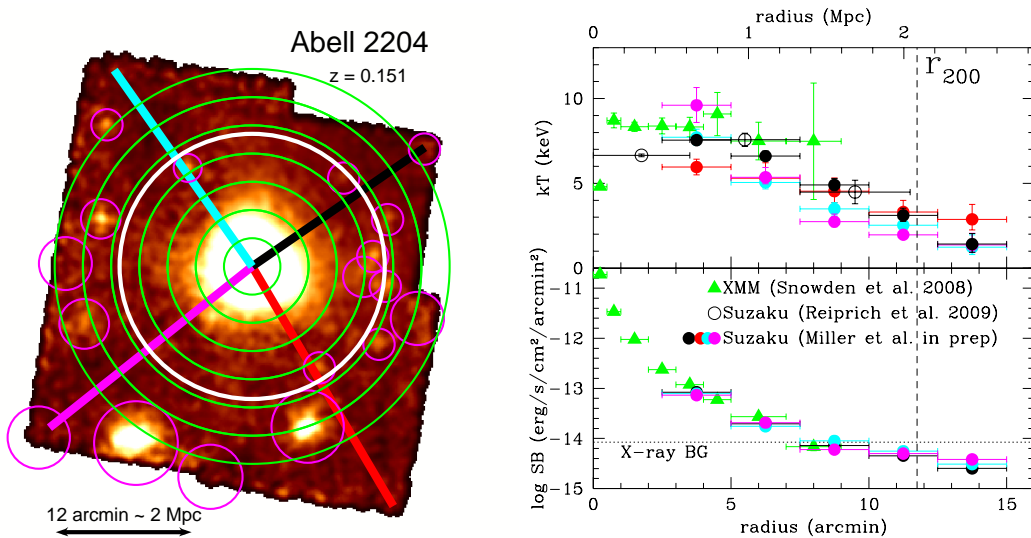


FIGURE 2. Abell 2204 0.5–2 keV combined, exposure-corrected *Suzaku* image (left) and profiles of temperature (right top) and surface brightness (right bottom). The profiles are measured in bins shown in the image by the green annuli, along radial directions with arrows corresponding to the colored points. The white circle shows $r_{200} = 2.3$ Mpc. Magenta circles identify point sources and other excised features in the X-ray image. The archival data from Reiprich et al. [14] are toward the northwest; those authors used different annuli than we have in the current analysis. The surface brightness profile has been background-subtracted, so that we clearly see excess emission beyond r_{200} ; however, the uncertainty is larger than shown here, as discussed in the text and in Figure 4.

THE POWER OF *SUZAKU*, *XMM*, AND *CHANDRA* TOGETHER

Suzaku, *XMM*, and *Chandra* together constitute an extremely powerful tool for understanding the outskirts of clusters. As noted above, *Suzaku*'s low background and substantial collecting area provide surface brightness sensitivity unavailable with other instruments. *XMM* and *Chandra* data provide high angular resolution that resolves the shape of the temperature profile near the cluster core, and excellent point source sensitivity in the cluster outskirts to minimize the effects of fluctuations in the background source density, as detailed below. Finally, comparison of the *XMM* and *Suzaku* data in the regions of overlap provide important cross-checks on systematic errors in temperature and flux at the very low surface brightness levels we hope to study.

For small extraction regions (~ 0.01 deg⁻²), fluctuations in the unresolved source background dominate the surface brightness uncertainty. For a typical 50 ksec exposure, we can expect to resolve and exclude sources from the *Suzaku* data alone down to a flux of about 10^{-13} erg cm⁻² s⁻¹. Assuming a differential source distribution along the lines of Moretti et al. [20], we expect surface brightness fluctuations in the 0.5–2 keV band to be $\sigma_B = 3.9 \times 10^{-12} \Omega_{0.01}^{-1/2}$ erg cm⁻² s⁻¹ deg⁻², where $\Omega_{0.01}$ is the region solid angle in units of 0.01 deg⁻² [9]. This is 30% of the typical X-ray background level measured in our Abell 1795 *Suzaku* background regions, and it accounts for 40% of the detected cluster emission at $r_{500} - r_{200}$ toward the north in Abell 1795 [9]. Including high spatial resolution data from *XMM* or *Chandra* allows us to remove fainter sources,

lowering our point source exclusion threshold by a factor of 10 in flux and reducing σ_B by a factor of ~ 3 –4. While increasing the solid angle will also mitigate fluctuations due to cosmic variance, we wish to trace azimuthal variations. This requires restricting extraction regions to at most a few times 0.01 deg^{-2} for the less extended clusters, and therefore we have required our *Suzaku* pointings to overlap as much as possible with available *XMM* or *Chandra* data so that we can adequately eliminate or model point sources.

These clusters generally lack *XMM* coverage in the outskirts, so we have begun a parallel project to obtain *Chandra* snapshot observations to fill in these regions. An example is illustrated in Figures 3 and 4. Including 5 ksec *Chandra* snapshots increases the number of detected point sources by an order of magnitude and reduces our surface brightness uncertainty by a factor of ~ 3 . For a given detected *Chandra* point source, we either exclude this source from the *Suzaku* extraction or include it as an additional component in the background fit, depending on the point source flux and size of the full extraction region. About one quarter of the *Chandra* observations are completed, and this analysis remains ongoing.

A CASE STUDY: THE OUTSKIRTS OF RXCJ 0605

The cluster RXCJ 0605.8-3518 (Abell 3378) appears to have a rising kT profile to r_{500} in the *XMM* analysis [12]. We present azimuthally-averaged, deprojected gas profiles from our *Suzaku* observations in Figures 5 and 6. The temperature decreases beyond the cluster core, as does the electron density, which is consistent with the *XMM* result in the overlap region and a $\beta = 0.68$ profile out well beyond r_{200} . The entropy profile increases steadily to as far as can be measured, in line with theoretical predictions [2] and at odds with results from previous clusters [e.g., Abell 1795; 9]. The gas fraction is fully consistent with the cosmic baryon fraction at large radius.

These results are also at odds with a recent study of the Perseus cluster [17, and elsewhere in these proceedings], which finds a flattening of the entropy profile (similar to other previous cluster studies) and an observed gas fraction well in excess of the baryon fraction near r_{200} . Such discrepancies with predictions can be explained by clumping of the ICM gas; since the X-ray emissivity is proportional to the square of the gas density, small dense regions will dominate the emission, biasing the entropy lower and the gas fraction higher compared to extrapolation from the more homogeneous inner regions. At this point, the importance of gas clumping near the virial radius remains unclear. The results from the Perseus cluster are clearly inconsistent with a homogeneous ICM in hydrostatic equilibrium, and clumping neatly explains the discrepancies between observations and predictions in the thermodynamic gas profiles. Clumping at various scales is also predicted by numerical simulations [3, 4, 21]. Yet our initial results and a recent *Suzaku* study of the fossil group RXJ 1159+5531 [22] are consistent with expectations from a homogeneous ICM and need not invoke clumping. To what extent environment, observing location (e.g., along a filament), or instrumental effects might play a role in these different results is an open question. Results from our full sample of clusters, as well as additional on-going studies of Perseus, Virgo, and other nearby bright clusters, will help solve this question.

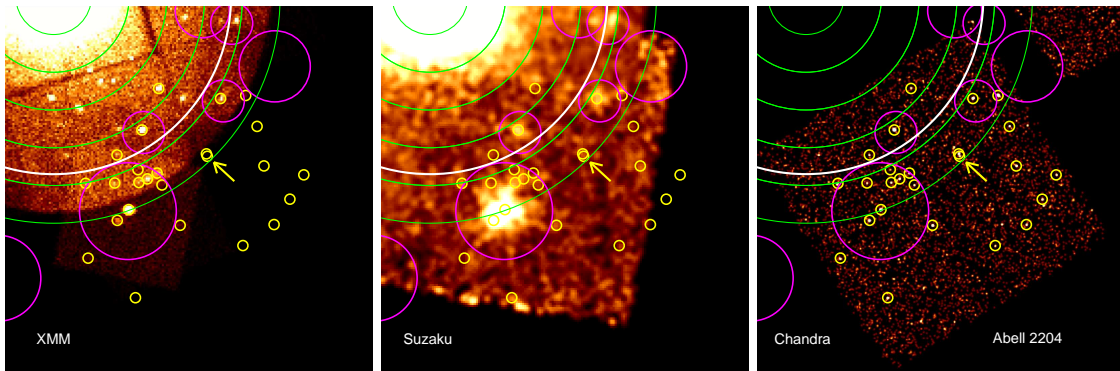


FIGURE 3. Images of the southwest quadrant of Abell 2204 from *XMM*, *Suzaku*, and *Chandra*, showing detected point sources from *Suzaku* (magenta circles) and *Chandra* (yellow circles). Other notations are described in Figure 2. The resolving power of *Chandra* allows detection of an order of magnitude more point sources than *Suzaku*, in an exposure one-eighth as deep. This depth allows tighter constraints on the cosmic background uncertainty, as discussed in the text and illustrated in Figure 4. The arrows indicate an example bright point source, detectable by *Chandra* but not *Suzaku*, which dominates the uncertainty in the outermost bin of Figure 4. Note that the very bright point source has very similar flux in each image, however due to the color scale and superior resolution it is less apparent in the *Chandra* image.

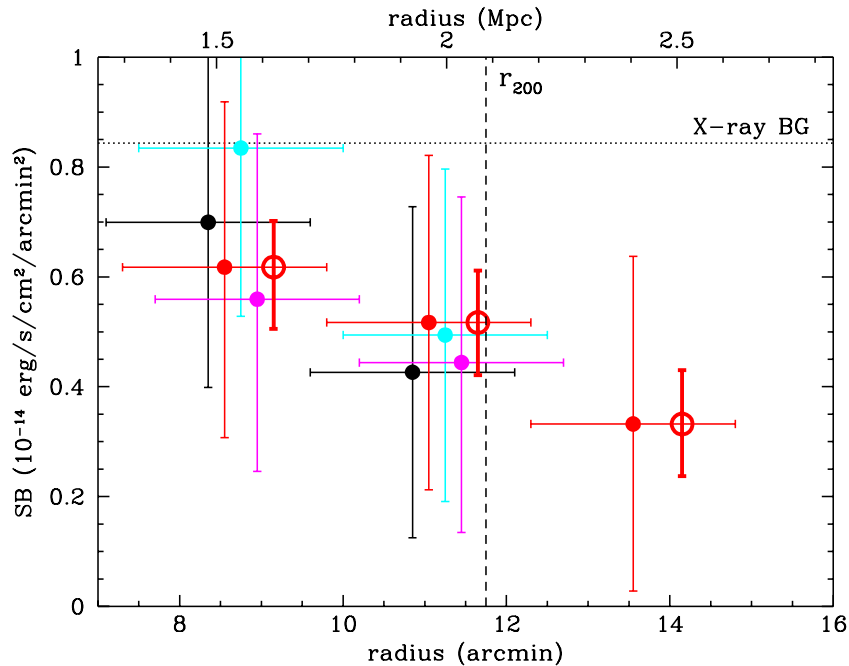


FIGURE 4. Zoom-in of the Abell 2204 background-subtracted surface brightness profile from Figure 2, showing only the outer three radial bins and with the ordinate plotted on a linear scale. The solid points have error bars that include the uncertainty due to unresolved point sources below the *Suzaku* flux limit. The open points include error down to the *Chandra* point source flux limit for the single *Suzaku* pointing (shown in Figure 3) with an overlapping *Chandra* snapshot. The uncertainty is lower by a factor of ~ 3 .

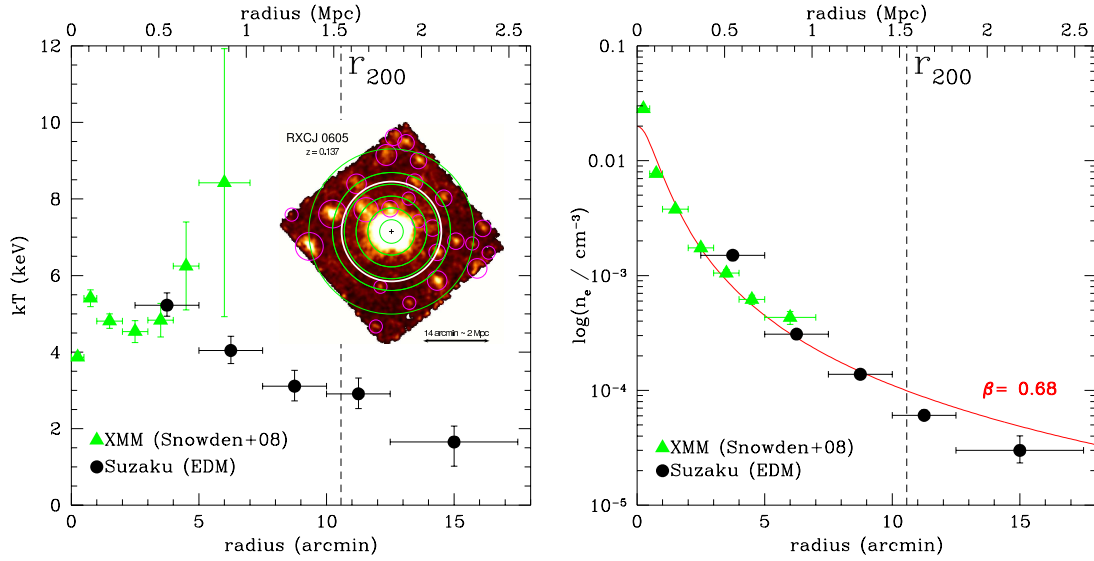


FIGURE 5. RXCJ 0605 temperature and electron density profiles. The inlay is the $0.5-2$ keV combined, exposure-corrected *Suzaku*/XIS image, with the same notations as in Figure 2.

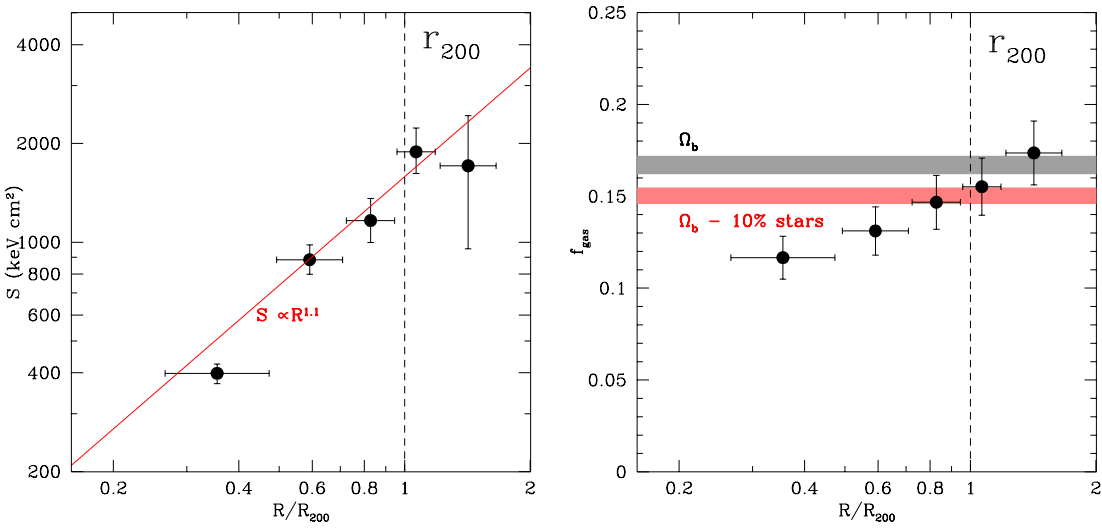


FIGURE 6. RXCJ 0605 entropy and f_{gas} profiles. The $S \propto R^{1.1}$ relation is from Voit [2]. The shaded regions in the f_{gas} plot show current estimates of the cosmic baryon fraction.

ACKNOWLEDGMENTS

We thank both the organizers and attendees of “*Suzaku* 2011” for a highly enlightening and enjoyable meeting. This work was supported by NASA grants NNX10AV02G and NNX09AE58G, and by SAO grant GO1-12165X.

REFERENCES

1. A. E. Evrard, C. A. Metzler, and J. F. Navarro, *ApJ* **469**, 494 (1996)
2. G. M. Voit, *Reviews of Modern Physics* **77**, 207 (2005)
3. M. Roncarelli, S. Ettori, K. Dolag, L. Moscardini, S. Borgani, and G. Murante, *MNRAS* **373**, 1339 (2006)
4. J. O. Burns, S. W. Skillman, and B. W. O’Shea, *ApJ* **721**, 110 (2010)
5. J. F. Navarro, C. S. Frenk, and S. D. M. White, *ApJ* **490**, 493 (1997)
6. S. Borgani, et al., *MNRAS* **348**, 1078 (2004)
7. A. Vikhlinin, et al., *ApJ* **692**, 1033 (2009)
8. S. W. Allen, R. W. Schmidt, H. Ebeling, A. C. Fabian, and L. van Speybroeck, *MNRAS* **353**, 457 (2004)
9. M. W. Bautz, et al., *PASJ* **61**, 1117 (2009)
10. A. Vikhlinin, et al., *ApJ* **692**, 1060 (2009)
11. G. W. Pratt, H. Böhringer, J. H. Croston, M. Arnaud, S. Borgani, A. Finoguenov, and R. F. Temple, *A&A* **461**, 71 (2007)
12. S. L. Snowden, R. F. Mushotzky, K. D. Kuntz, and D. S. Davis, *A&A* **478**, 615 (2008)
13. M. R. George, A. C. Fabian, J. S. Sanders, A. J. Young, and H. R. Russell, *MNRAS* **395**, 657 (2009)
14. T. H. Reiprich, et al., *A&A* **501**, 899 (2009)
15. A. Hoshino, et al., *PASJ* **62**, 371 (2010)
16. M. Kawaharada, et al., *ApJ* **714**, 423 (2010)
17. A. Simionescu, et al., *Science* **331**, 1576 (2011)
18. H. Akamatsu, A. Hoshino, Y. Ishisaki, T. Ohashi, K. Sato, Y. Takei, and N. Ota, *PASJ*, submitted (2011), [astro-ph/1106.5653](#)
19. A. M. Juett, D. S. Davis, and R. Mushotzky, *ApJ* **709**, L103 (2010)
20. A. Moretti, S. Campana, D. Lazzati, and G. Tagliaferri, *ApJ* **588**, 696 (2003)
21. D. Nagai, and E. T. Lau, *ApJ* **731**, L10 (2011)
22. P. J. Humphrey, D. A. Buote, F. Brighenti, H. M. L. G. Flohic, F. Gastaldello, and W. G. Mathews, *ApJ*, submitted (2011), [astro-ph/1106.3322](#)